©2006. **Ya. L. Bogomolov, E. S. Semenov, A. D. Yunakovsky**

SCATTERING OF ELECTROMAGNETIC WAVES IN AN ACCELERATING SECTION OF A SUPERCOLLIDER

A problem of synthetizing of an optimal accelerating section for electron-positron colliders is considered. A boundary surface shape for such an electrodynamical system, which provides a stable structure of electromagnetic fields required, is suggested. Wave scattering in the system synthesized is investigated on the basis of the method of discrete sources. Some recommendations concerning optimization of boundary shapes are proposed.

Keywords and phrases: accelerating section of a supercollider, scattering problem, method of discrete sources.
MSC (2000): 35Q60

Introduction.

Designing of linear accelerators for novel electron-positron colliders is based on using of a high-frequency pumping [1]. Such an approach is based on the fact that the accelerating gradient (the value of the particle-synchronous harmonic of an electric field) may be increased only proportionally to a drive frequency [2]. Therefore, it is inevitable to use quasioptical components. The basic motivations and restrictions when synthesizing quasioptical structures for electron-positron colliders are formulated in [3]. A proper structure presented ibidem is a periodic set of coaxial radial-corrugated metal discs (two neighbor discs compose a Bragg reflection cavity) which is fed with a wave flow converging onto the structure axis (Fig. 1). An optimization problem is considered as follows. For fixed the accelerating gradient, the drive frequency and the accelerating channel inner diameter it is required to synthesize a structure, where minimum RF energy would be accumulated within the channel and minimization of electric field maximum on metal discs would be realized at the same time.

This optimization problem generates some model ones [4]–[7]. One of them is an external scattering problem for an infinite domain in the azimuth-symmetrical case. The previous results [4]–[6] concerning shapes of boundary surfaces for both a paraxial volume and Bragg cavities are exploited. Besides, a shape of a boundary surface for an outside volume, which can suppress spurious modes [8], is discussed here. A mathematical model is presented in Section 1.

Numerical algorithms are described in Section 2. They are based on the method of discrete sources (MDS) [9]. The knot of this method is the way of source placement. Much attention is paid to this question. Another algorithmic basis is the singular value decomposition (SVD) technique [10]. SVD gives a clear diagnosis how close to resonance the situation is. Moreover, the eigenvector corresponding to zero eigenvalue (resonance case) is produced immediately by SVD.

The primary results of numerical experiments for various combinations of boundary surfaces are presented in Section 3.

1. Mathematical model.

For 3D azimuth-symmetrical case the scattering problem is described by a scalar equation of Helmholtz type for the azimuth component of a magnetic field H_φ (wave number κ is

normalized to unity):

$$\Delta H_\varphi + \left(1 - \frac{1}{r^2}\right) H_\varphi = 0, \tag{1}$$

where $\Delta = \left(\frac{\partial^2}{\partial z^2} + \frac{\partial^2}{\partial r^2} + \frac{1}{r}\frac{\partial}{\partial r}\right)$ is Laplacian in the azimuth-symmetrical case, r and z are the radial and the axial (longitudinal) coordinates correspondingly.

The problem is considered in the infinite strip

$$0 \le r \le \infty, \quad 0 \le z \le \pi \tag{2}$$

less the internal domain restricted by the curve

$$S(r, z) = 0, \tag{3}$$

which is the equation of a longitudinal cross-section of an elementary disc (Fig. 2).

The boundary conditions reflect:

1) equality to zero of the tangential component of an electric field on a metal surface (3)

$$-i\,\overrightarrow{E_\tau} = \left(\text{rot}\ \overrightarrow{H_\varphi}\right)_\tau \equiv -\frac{\partial S}{\partial z}\left(-\frac{\partial H_\varphi}{\partial z}\right) + \frac{\partial S}{\partial r}\left[\frac{1}{r}\frac{\partial (r\,H_\varphi)}{\partial r}\right] = 0; \tag{4}$$

2) symmetry and periodicity of the structure in the z coordinate

$$\frac{\partial H_\varphi}{\partial z} = 0 \qquad \text{at} \quad z = 0, \pi; \tag{5}$$

3) equality to zero of the azimuth component of a magnetic field on the structure axis

$$H_\varphi = 0 \qquad \text{at} \quad r = 0. \tag{6}$$

In the case of azimuth symmetry both the axial component of an electric field E_z and the radial one E_r are expressed explicitly in terms of the azimuth component of a magnetic field H_φ:

$$-i\,E_z = \frac{\partial H_\varphi}{\partial r} + \frac{1}{r} H_\varphi, \tag{7}$$

$$-i\,E_r = -\frac{\partial H_\varphi}{\partial z}. \tag{8}$$

An incident wave $H_{\varphi\,\text{in}}$ is assumed to be the convergent cylindrical wave

$$H_{\varphi\,\text{in}}(r) = \frac{i}{4} H_1^{(2)}(r). \tag{9}$$

The boundary condition (6) generates a regular part of the scattering solution, which is the divergent cylindrical wave:

$$H_{\varphi\,\text{reg}}(r) = \frac{i}{4} H_1^{(1)}(r). \tag{10}$$

Here, in Eqs.(9)–(10), $H_1^{(1)}$ and $H_1^{(2)}$ are the Hankel functions.

The boundary curve (3) generates an additional scattering wave $H_{\varphi\,\mathrm{add}}(r,z)$, finding of which is the essence of the scattering problem. So, an unknown solution H_φ is sought as a sum of the incident wave and the scattering one:

$$H_\varphi = H_{\varphi\,\mathrm{in}} + H_{\varphi\,\mathrm{scat}}; \tag{11}$$

in its turn, $H_{\varphi\,\mathrm{scat}}$ represents a sum of two components

$$H_{\varphi\,\mathrm{scat}} = H_{\varphi\,\mathrm{reg}} + H_{\varphi\,\mathrm{add}}. \tag{12}$$

For the sake of uniqueness, $H_{\varphi\,\mathrm{scat}}$ must to be divergent in infinity, i. e., it satisfies the radiation condition

$$\frac{\partial H_{\varphi\,\mathrm{scat}}}{\partial r} - iH_{\varphi\,\mathrm{scat}} = O\left(\frac{1}{r}\right) \qquad \text{at} \quad r \to \infty. \tag{13}$$

Eqs.(1)–(13) represent the mathematical model for the accelerating section of a collider, which is fed with the cylindrical wave flow converging onto the structure axis.

Let us pay brief attention to elements of the boundary profile (3).

The axial component of an electric field E_z in the paraxial domain is required to be the cosine standing wave

$$E_z = 2\,C\cos z, \tag{14}$$

where C is the constant. The boundary condition (4) (perpendicularity of an electric field to a highly conductive metal surface) may be written in the form

$$E_r\,dr + E_z\,dz = 0, \tag{15}$$

where dr and dz are the components of a vector tangent to the metal surface. With use of Eqs.(7)–(8) the equation (15) yields

$$r\,dr = -2\,\mathrm{ctg}\,z\,dz, \tag{16}$$

the solution of which is the surface preserving an electric field in the form of the standing wave (14)

$$r^2 = r_1^2 - 4\ln\sin z, \tag{17}$$

where r_1 is the width of the accelerating channel (Fig. 2). Note, that in this case the azimuth component of a magnetic field H_φ and the radial component of an electric field E_r are (see (7), (8), (14)):

$$H_\varphi = -i\,C\,r\cos z, \tag{18}$$

$$E_r = C\,r\sin z. \tag{19}$$

In a similar way it is shown, that the boundary surface

$$r = const \tag{20}$$

ensures correctness of the boundary condition (4) for the solution

$$H_\varphi = \frac{C}{r}\cos z. \tag{21}$$

It means the appearance of a spurious mode in the outside part of the system considered. This spurious mode takes away the energy of the incident wave from the paraxial domain. Therefore, the boundary surface of the outside volume should not be chosen in the form (20). To suppress the spurious mode, it is recommended to use a profile (17) shifted by $\frac{\pi}{2}$ along the z coordinate. This profile must form in the outside volume the mode

$$H_\varphi = C\, r \cos(z - \pi/2) = C\, r \sin z, \tag{22}$$

which is impossible at $r \gg 1$ according to energy reasons.

The complete profile of the elementary disk recommended for the accelerating structure is shown in Fig. 2. It is obtained by connection of the contours of paraxial and outside volumes by narrow channels with asymmetric grooves (for amplification of the standing wave on the structure axis). The optimal parameters for two neighboring channels in the case of plane geometry are obtained in [5]. For the case of cylindrical geometry these parameters are defined more exactly using the numerical procedure. Note, that, despite of a priori considerations and numerous numerical experiments, the question on synthesis of optimal paraxial (17) and outside (22) volumes is still open.

2. Numerical algorithms.

To find an approximate solution of the problem (1)–(13) the method of discrete sources (MDS) is used [9]. An unknown function $H_{\varphi\,\mathrm{add}}$ is sought in the form

$$H_{\varphi\,\mathrm{add}}(r, z) = \sum_{i=1}^{N} d_i\, G(r, z, \rho_i, \zeta_i), \tag{23}$$

where $G(r, z, \rho_i, \zeta_i)$ is the Green function of the operator considered (1), (5), (6), (13) in the envelope domain (2), d_i are the amplitudes of sources, ρ_i, ζ_i are the source coordinates, N is the number of sources used.

The Green function $G(r, z, \rho, \zeta)$ may be presented as an expansion into one-dimensional eigenfunctions either in the radial coordinate r (cylindrical functions) or in the longitudinal coordinate z (trigonometric functions). Both representations yield one and the same result, however, the trigonometric representation demonstrates faster convergence, that is why preference is given to it:

$$G(r, z, \rho, \zeta) = -\frac{i}{4} G_0(r, \rho) - \frac{1}{\pi} G_1(r, \rho) \cos z \cos \zeta - \frac{i}{2} \sum_{n=2}^{\infty} G_n(r, \rho) \cos(nz) \cos(n\zeta). \tag{24}$$

Here, for $r < \rho$

$$G_0(r, \rho) = H_1^{(1)}(\rho) \left[H_1^{(1)}(r) + H_1^{(2)}(r) \right], \quad G_1(r, \rho) = r/\rho,$$

$$G_n(r, \rho) = H_1^{(1)}(i\lambda_n \rho) \left[H_1^{(1)}(i\lambda_n r) + H_1^{(2)}(i\lambda_n r) \right],$$

where $H_1^{(1)}$, $H_1^{(2)}$ are the Hankel functions, $\lambda_n = \sqrt{n^2 - 1}$. For $r > \rho$ the variables r and ρ change places in the right hand side of (24) (symmetry property of the Green function).

Taking into account the properties of the Green function (24) and functions (9)–(10), the unknown function H_φ (11) satisfies the equation (1) together with the boundary conditions

(5)–(6) as well as its scattering component $H_{\varphi\,\mathrm{scat}}$ satisfies the scattering condition (13). Substituting (11) into Eq. (4) (with use of (9), (10) and (23)) for all collocation points (points, where the validity of the boundary condition (4) is verified) on the boundary surface (3) we arrive at a set of linear algebraic equations (SLAE) for unknown values of source amplitudes d_i:

$$\sum_{i=1}^{N} d_i \left\{ \left[\frac{\partial G}{\partial r}(r_j, z_j, \rho_i, \zeta_i) + \frac{1}{r_j} G(r_j, z_j, \rho_i, \zeta_i) \right] \cos\beta_j - \right.$$
$$\left. - \frac{\partial G}{\partial z}(r_j, z_j, \rho_i, \zeta_i) \sin\beta_j \right\} = -\frac{i}{2} J_0(r) \cos\beta_j \quad j = \overline{1, N}, \tag{25}$$

where $\mathrm{tg}\,\beta = r'(s)/z'(s)$, $(r(s), z(s))$ is the parametric representation of the boundary surface (3), $J_0(r)$ is the Bessel function. The values d_i obtained from (25) determine the approximate solution of the scattering problem.

Allocation of sources and collocation points is the problem of great importance. The practical experience gives the basic recipes, which are as follows (Fig. 3). The collocation points may be allocated uniformly along the boundary. On the smooth pieces of the boundary the rarefaction of them (pieces 2, 5, 8 in Fig. 3) and even their complete absence (piece 1 in Fig. 3 — one more remarkable property of the curve (17)) is allowed. At the same time, in neighborhoods of the exterior angular points (A, B, C in Fig. 3) their accumulation is required. Moreover, the double verification of the boundary condition (4) at the angular points (A, B, C, D, E in Fig. 3) seems to be natural because of two tangent directions at these points.

In the neighborhood of any exterior angular point (A, B or C in Fig. 3) there is a pole point. A source being allocated at this point, SLAE (25) becomes degenerate [11]. The sources here should be disposed on a curve (e.g., uniformly on a circle) bordering the singular point. In that case a fractional singularity is simulated correctly [11], [12]. Basically, it is enough to use four source points. To make accuracy higher, the number of sources should be increased in the neighborhoods of singular points.

For the sake of better convergence of series in Eq. (24) coordinates of sources and collocation points should differ from each other in both the radial r and the longitudinal z variables. One possible variant is the placement of sources at the tops of isosceles triangles, other tops of which are neighboring collocation points on the boundary (Fig. 3). The height of triangles is a free parameter h.

The above-stated recipes allows to use ~ 10 points for simple boundaries (Fig. 4) and ~ 100 points for boundaries of complicated shapes (Fig. 5, 6).

To obtain a resonance solution, it is necessary to fit a boundary surface of the system synthesized to the shape ensuring zero eigenvalue. A numerical procedure is needed, which, firstly, diagnoses presence of zero eigenvalue, and, secondly, selects the eigenfunction corresponding to it from a solution. For these purposes there exists a powerful technique known as singular value decomposition (SVD) [10].

First of all, SVD gives a clear diagnosis of the situation: how close to singular the matrix is. Moreover, SVD solves effectively a set of homogeneous linear algebraic equations (SHLAE) $Ax = 0$ in the case that the matrix A is singular. The solution is obtained immediately by means of SVD:

$$A = UWV^T, \qquad U^T U = V^T V = I, \tag{26}$$

where U and V are the orthogonal matrices, W is the diagonal matrix with nonnegative

elements (the singular values), I is the identity matrix. Any column of V, whose corresponding element of W is zero yields a solution of SHLAE. At last, application of SVD to SLAE with a nonzero right hand side is useful too. In fact, SVD obtains explicitly both the resonance component and the "range" (nonresonance) one. That is especially useful in the situation, where several eigenvalues are nearly zero.

The constructive algorithm for finding of resonance domains for the operator (1) together with the boundary conditions (4)–(6) and an artificial metal at some value in the radial coordinate $r = r_2$ is presented in [4]. In particular, a remarkable property of the curve (17) (one more additional argument in its favour) had been verified numerically: it forms an "infinite" resonator with the mode (18), if $r \to \infty$ [4]. Indeed, since the function (18) is quadratic summable inside a complete volume of the "infinite" resonator, it is the eigenfunction of the discrete spectrum of the operator (1), (4)–(6) corresponding to zero eigenvalue.

Analytical considerations, numerical algorithms and results obtained earlier (see [4]–[7], [11]) are exploited for the complete external scattering problem (1)–(13).

3. Numerical results.

The prime test for the numerical algorithm (23)–(26) is as follows. A closed boundary surface (3) in the scattering problem (1)–(13) being an arbitrary combination of straight lines (here r_{0i} is the i-th zero of the Bessel function $J_0(r)$, z_j is the arbitrary number from the interval $(0, \pi/2)$),

$$r = r_{0i} \qquad \text{and} \quad z = z_j, \tag{27}$$

the scattering is absent at all, i. e., a free propagation of the cylindrical wave is realized (Fig. 4)

$$H_\varphi = J_1(r), E_z = J_0(r), E_r \equiv 0. \tag{28}$$

A qualitative coincidence of a numerical solution with the exact one (28) in the radial coordinate is obtained. At the same time the numerical solution is homogeneous in the axial coordinate. As for a quantitative comparison, the relative mean square error is approximately equal to 0.1 % even for a small number (~ 20) of sources used. The similar results for other domains are obtained.

The main results of other numerical experiments are as follows.

To obtain the homogeneous (in the radial direction) axial component of an electric field E_z with a large projection onto the harmonic synchronous to relativistic particles, it is enough to use asymmetric shapes for the paraxial volume (Fig. 5). However, without grooves (symmetric or asymmetric) in channels connecting the paraxial profile with the outside one it is impossible to obtain a considerable magnitude of the accelerating gradient. As well as it is impossible to suppress the spurious mode (21) in the outside volume. It is well seen (Fig. 5), that a magnetic field in the outside volume (contrary to the incident wave (9)) is inhomogeneous in the longitudinal coordinate z.

The best results are obtained for the contour drawn in Fig. 6. This contour is as follows:
1) the paraxial part is chosen in the form (17);
2) the outside part is chosen in the same form shifted by $\frac{\pi}{2}$ in the z coordinate;
3) asymmetric Bragg reflectors with parameters obtained in [5] (they are defined more accurately for the cylindrical case) connecting the paraxial part with the outside one.

This contour provides in the paraxial volume a stable (with respect to changes of the contour parameters) homogeneous standing wave with essentially higher amplitude in

comparison with the incident cylindrical wave. Besides, it essentially suppresses the spurious mode of a magnetic field in the outside volume, where the homogeneous incident wave (9) plays the basic part.

4. Summary.

This paper continues a series of works published earlier [4]–[7], [11]. To synthesize an optimal accelerating section for electron-positron colliders, some model problems of a various type (boundary, spectral, scattering) are solved. The numerical algorithms based on the method of discrete sources and the singular value decomposition technique are developed. The shapes of boundary surfaces of metal disks ensuring fields in electrodynamical systems with properties required are obtained.

Acknowledgements.

Authors wish to express gratitude to professor M. I. Petelin for fruitful discussions and reasonable advice.

Appendix. Figures.

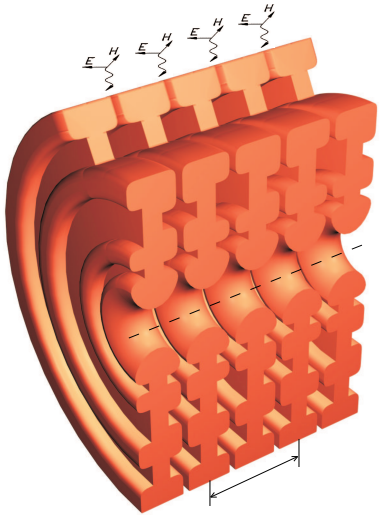

Fig.1. *Quasi-optical electron accelerator (λ is the period of a structure = a wave length).*

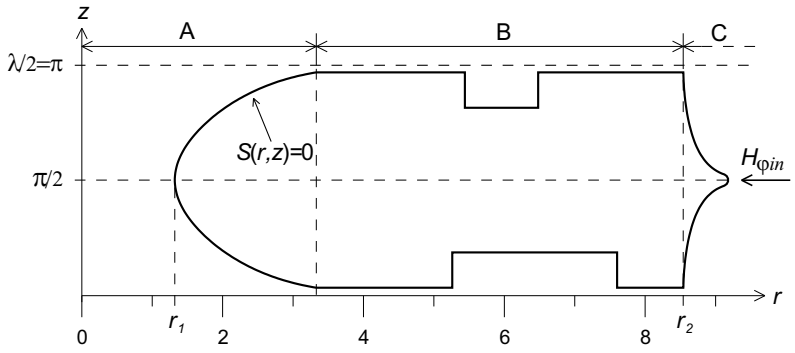

Fig. 2. *The external scattering problem (1)–(13) (A is the paraxial volume, B are the channels with different Bragg reflectors, C is the external volume; the incident wave $H_{\varphi\,\mathrm{in}}(r) = \frac{i}{4}H_1^{(2)}(r)$; $H_1^{(2)}(r)$ is the Hankel function; λ is the wave length).*

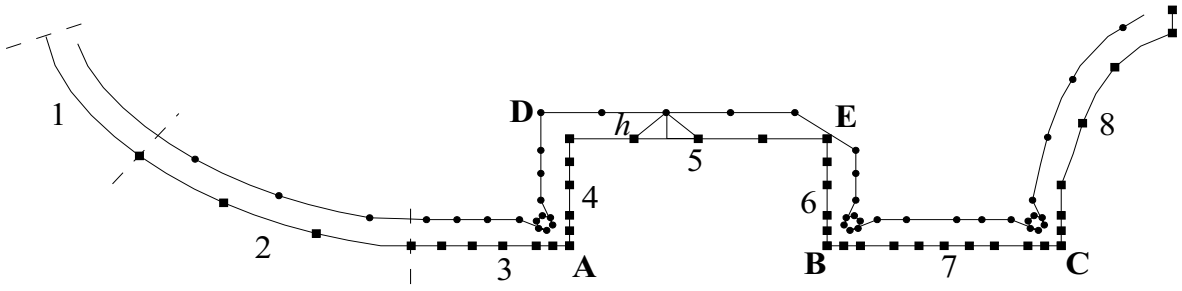

Fig. 3. *Allocation of sources (circles) and collocation (squares) points.*

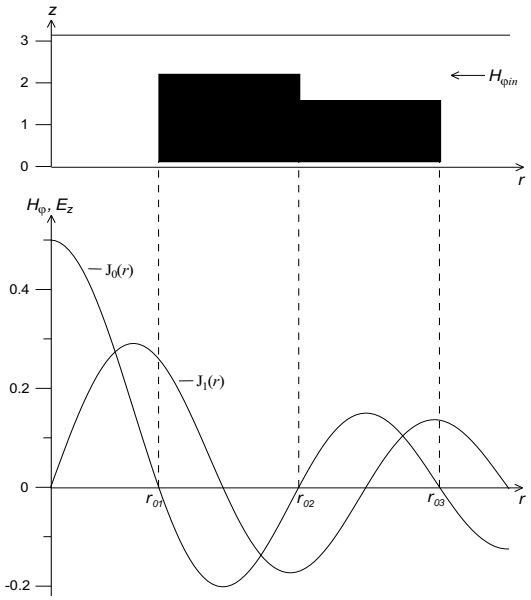

Fig. 4. *Test scattering problem (1)–(13) without scattering on a metal shape (3). The exact solution is* $H_\varphi = J_1(r)$, $E_z = J_0(r)$ $(E_r \equiv 0)$*; here* r_{01}, r_{02}, r_{03} *are the zeroes of the Bessel function* $J_0(r)$*; the incident wave is the Hankel function* $H_{\varphi\,\mathrm{in}}(r) = \frac{i}{4}H_1^{(2)}(r)$.

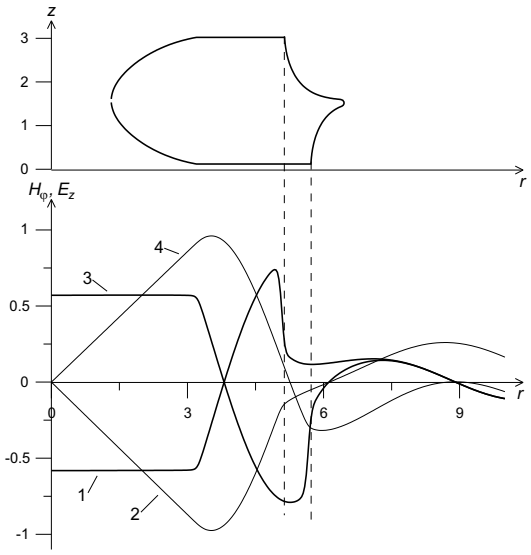

Fig. 5. *Asymmetric profile without Bragg reflectors. The curves 1, 2 correspond to electric and magnetic fields at* $z = \pi$*; curves 3, 4 — at* $z = 0$.

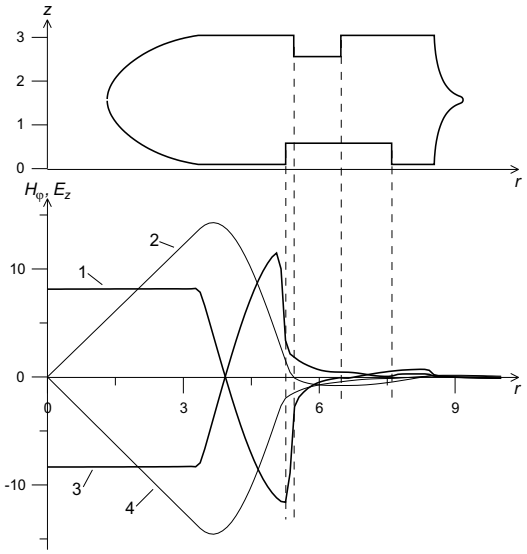

Fig. 6. *Profile of a metal disk providing the best properties of fields in the system. The curves 1, 2 correspond to electric and magnetic fields at $z = \pi$; curves 3, 4 — at $z = 0$.*

1. *Petelin M. I.* Quasi-optical Collider Concept // Proceedings of the Advanced Accelerator Concepts, Tenth Workshop, 2002, pp. 459–468.
2. *Wilson P. B.* Application of High Power Microwave Sources to TeV Linear Colliders // Applications of High Power Microwaves / Ed. by A. V. Gaponov-Grekhov, V. L. Granatstein, Boston, London: Artech House, 1994, pp. 229–317.
3. *Petelin M. I.* Quasi-optical Electron-positron Colliders? // Strong Microwaves in Plasmas, Proceedings of the Int. Workshop / Ed. by A. G. Litvak, N. Novgorod, 2003.- Vol. 1,- pp. 82–89.
4. *Bogomolov Ya. L., Semenov E. S. & Yunakovsky A. D.* Singular value decomposition as a tool for solving of spectral problems arisen in supercollider simulation // Proceedings of the International Seminar "Day on Diffraction — 2003", Saint Petersburg: Universitas Petropolitana, 2003, pp. 22–31.
5. *Bogomolov Ya.L., Petelin M.I., Tai M.L. & Yunakovsky A.D.* Synthesis of Bragg Reflectors for Electron Accelerating Structures with Quasi-Optical Feed // Radiophysics and Quantum Electronics, 2003. Vol. 46, № 5–6, pp. 425–433.
6. *Bogomolov Ya. L. & Yunakovsky A. D.* Simulation of Electrodynamical Systems of Energy Accumulation // Modern methods in the theory of boundary problems, Proc. of Voronezh spring mathematical school "Pontryagin readings-XI", Voronezh, VGU, 2000 Vol. 1, pp. 37–47 (in Russian).
7. *Bogomolov Ya. L., Semenov E. S. & Yunakovsky A. D.* Method of discrete sources for elliptic problems arising in supercollider simulation // Nonlinear Boundary Problems, Donetsk, 2005. Vol. 15, pp. 31–40.
8. *Kamotsky I. V., Nazarov S. A.* Wood anomalies and surface waves in a scattering problem on a periodic boundary // Mat. Sbornik, 1999.- Vol. 190, № 1, pp. 109–138 (in Russian).
9. *Eremin Yu. A. & Sveshnikov A. G.* Method of Discrete Sources in Electromagnetic Diffraction Problems // M.: izd-vo MGU, 1992 (in Russian).
10. *Demmel J. W.* Applied Numerical Linear Algeba // Philadelphia: SIAM, 1997.
(*Demmel Dzh.* Vychislitel'naya lineinaya algebra. Teoriya i prilozheniya // M.:Mir, 2001.)
11. *Bogomolov Ya.L. & Yunakovsky A.D.* Scattering of Electromagnetic Waves in a Collider Channels // Nonlinear Boundary Problems, Donetsk, 2003.- Vol. 13, pp. 18–30.
12. *Samko S. G., Kilbas A. A. & Marichev O. I.* Integrals and derivatives of the fractional order and their applications // Minsk: Nauka I Tekhnika, 1987 (in Russian).

Institute of Applied Physics Russian Academy of Sciences
46 Uljanov Street, Nizhny Novgorod, 603950, Russia
bogomol@appl.sci-nnov.ru
semes@appl.sci-nnov.ru
yun@appl.sci-nnov.ru

Received 14.12.2005